MATHEMATICAL COMMUNICATIONS
Math. Commun. **19**(2014), 1–28

Spherical folding tessellations by kites and isosceles triangles: a case of adjacency

Catarina Pina Avelino[1] and Altino Manuel Folgado dos Santos[1,*]

[1] *Universidade de Trás-os-Montes e Alto Douro, UTAD, Quinta de Prados, 5 001-801 Vila Real, Portugal*

Received August 13, 2012; accepted September 27, 2013

Abstract. The classification of dihedral folding tessellations of the sphere and the plane whose prototiles are a kite and an equilateral triangle are obtained in a recent paper, [1]. In this paper, we extend this classification presenting all the dihedral folding tessellations of the sphere by kites and isosceles triangles in a particular case of adjacency. A list containing these tilings including its combinatorial structure is presented in Table 1.

AMS subject classifications: 52C20, 05B45, 52B05

Key words: dihedral f-tilings, combinatorial properties, spherical trigonometry, symmetry groups

1. Introduction

By a *folding tessellation* or *folding tiling* of the sphere S^2 we mean an edge-to-edge pattern of spherical geodesic polygons that fills the whole sphere with no gaps and no overlaps such that the "underlying graph" has even valency at any vertex and the sums of alternate angles around each vertex are π.

Folding tilings are strongly related to the theory of isometric foldings on Riemannian manifolds. In fact, the set of singularities of any isometric folding corresponds to a folding tiling, see [10] for the foundations of this subject.

The study of these special class of tessellations was initiated in [2] with a complete classification of all spherical monohedral folding tilings. Ten years latter, Ueno and Agaoka [11] have established the complete classification of all triangular spherical monohedral tilings (without any restriction on angles).

Dawson has also been interested in special classes of spherical tilings, see [7], [8] and [9], for instance.

The complete classification of all spherical folding tilings by rhombi and triangles was obtained in 2005 [5]. A detailed study of triangular spherical folding tilings by equilateral and isosceles triangles is presented in [6].

Spherical f-filings by two non congruent classes of isosceles triangles have been recently obtained [3].

Here we discuss dihedral folding tessellations by spherical kites and spherical isosceles triangles.

*Corresponding author. *Email addresses:* cavelino@utad.pt (C. P. Avelino), afolgado@utad.pt (A. F. Santos)

A spherical kite K (Figure 1(a)) is a spherical quadrangle with two congruent pairs of adjacent sides, but distinct from each other. Let us denote by $(\alpha_1, \alpha_2, \alpha_1, \alpha_3)$, $\alpha_2 > \alpha_3$, the internal angles of K in cyclic order. The length sides are denoted by a and b, with $a < b$. From now on, T denotes a spherical isosceles triangle with internal angles β and γ ($\gamma \neq \beta$), and length sides c and d, see Figure 1(b).

By $\Omega(K, T)$ we shall denote the set, up to isomorphism, of all dihedral folding tilings of S^2 whose prototiles are K and T.

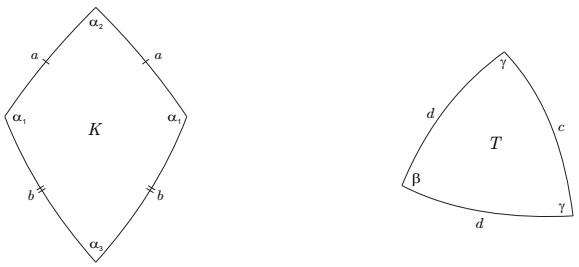

(a) (b)

Figure 1: *A spherical kite and a spherical isosceles triangle*

Taking into account the area of the prototiles K and T we have

$$2\alpha_1 + \alpha_2 + \alpha_3 > 2\pi \quad \text{and} \quad \beta + 2\gamma > \pi.$$

As $\alpha_2 > \alpha_3$, we also have

$$\alpha_1 + \alpha_2 > \pi.$$

After certain initial assumptions are made, it is usually possible to deduce sequentially the nature and orientation of most of the other tiles. Eventually, either a complete tiling or an impossible configuration proving that the hypothetical tiling fails to exist is reached. In the diagrams that follow, the order in which these deductions can be made is indicated by the numbering of the tiles. For $j \geq 2$, the location of tiling j can be deduced directly from the configurations of tiles $(1, 2, \ldots, j-1)$ and from the hypothesis that the configuration is part of a complete tiling, except where otherwise indicated.

We begin by pointing out that any element of $\Omega(K, T)$ has at least two cells congruent to K and T, respectively, such that they are in adjacent positions and in one and only one of the situations illustrated in Figure 2.

In this paper we consider the first case of adjacency.

2. Case of adjacency I

Suppose that any element of $\Omega(K, T)$ has at least two cells congruent to K and T, respectively, such that they are in adjacent positions, as illustrated in Figure 2–I. As $a = d$, using trigonometric formulas, we obtain

$$\frac{\cos\gamma\,(1+\cos\beta)}{\sin\gamma\sin\beta} = \frac{\cos\frac{\alpha_3}{2} + \cos\alpha_1\,\cos\frac{\alpha_2}{2}}{\sin\alpha_1\,\sin\frac{\alpha_2}{2}}. \tag{1}$$

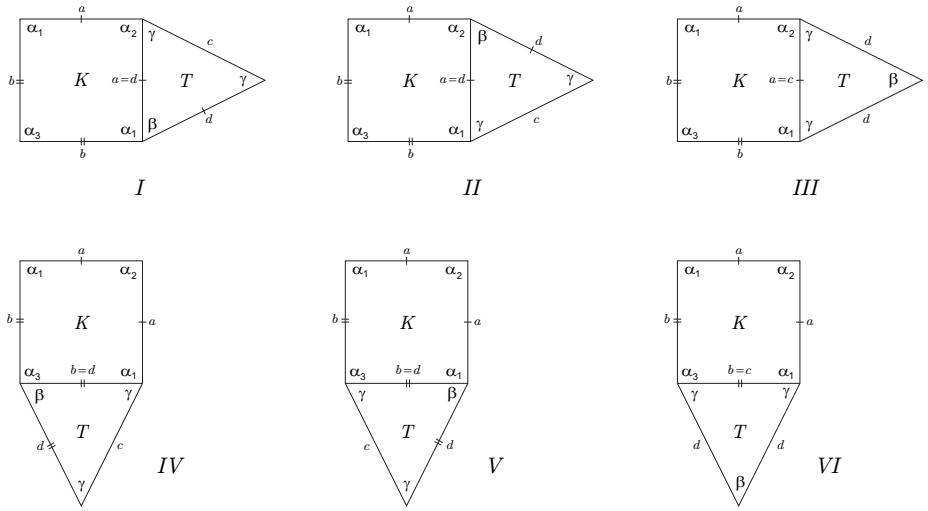

Figure 2: *Distinct cases of adjacency*

Concerning the angles of the triangle T, we have necessarily one of the following situations:

$$\gamma > \beta \quad \text{or} \quad \gamma < \beta.$$

In the following subsections we consider each of these cases separately. The results will show that there are no f-tilings for both instances.

2.1. $\gamma > \beta$

As $\gamma > \beta$, we have $\gamma > \frac{\pi}{3}$ and $c < a = d < b$, i.e., all the lengths are pairwise distinct (except a and d). Concerning the angles of the kite K, we have necessarily one of the following situations: $\alpha_1 \geq \alpha_2 > \alpha_3$ or $\alpha_2 > \alpha_1, \alpha_3$ (includes the cases $\alpha_2 > \alpha_1 \geq \alpha_3$ and $\alpha_2 > \alpha_3 > \alpha_1$).

The propositions that follow address these distinct conditions.

Proposition 1. *If $\alpha_1 \geq \alpha_2 > \alpha_3$, then $\Omega(K,T)$ is an empty set.*

Proof. Suppose that any element of $\Omega\,(K,T)$ has at least two cells congruent to K and T, respectively, such that they are in adjacent positions, as illustrated in Figure 2$-I$ and $\alpha_1 \geq \alpha_2 > \alpha_3$ $\left(\alpha_1 > \frac{\pi}{2}\right)$. With the labeling of Figure 3(a), we have

$$\theta_1 = \gamma \quad \text{or} \quad \theta_1 = \beta.$$

1. Suppose firstly that $\theta_1 = \gamma$. At vertex v_1 we cannot have $\alpha_1 + \gamma = \pi$, otherwise there is no way to satisfy the angle-folding relation around this vertex. On the other hand, if $\alpha_1 + \gamma < \pi$, it follows that $\gamma < \frac{\pi}{2} < \alpha_1$ and $\alpha_1 + \gamma + k\alpha_3 = \pi$, $k \geq 1$ (see Figure 3(b)), as $\alpha_1 + \gamma + \beta > \pi$ and $\beta < \gamma < \alpha_2 \leq \alpha_1$. Again, there is no way to satisfy the angle-folding relation around vertex v_1.

2. Suppose now that $\theta_1 = \beta$ (Figure 4(a)). If $\gamma < \frac{\pi}{2}$, as illustrated in Figure 4(b),

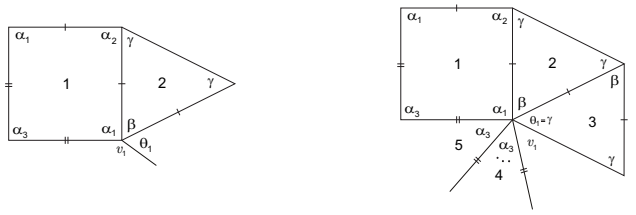

(a) (b)

Figure 3: *Local configurations*

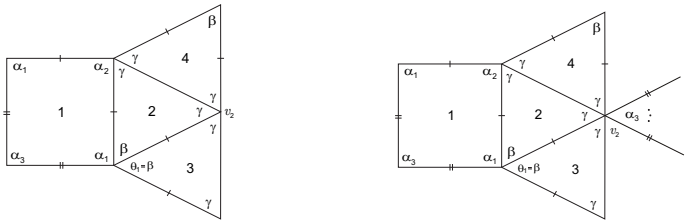

(a) (b)

Figure 4: *Local configurations*

there is no way to satisfy the angle-folding relation around vertex v_2 (note that $\alpha_2 > \beta$). Thus, $\gamma = \frac{\pi}{2}$ and

$$\alpha_1 > \frac{\pi}{2} = \gamma \geq \alpha_2 > \alpha_3, \beta.$$

Now, we consider separately the cases $\alpha_2 = \frac{\pi}{2}$ and $\alpha_2 < \frac{\pi}{2}$.

2.1. Suppose that $\alpha_2 = \frac{\pi}{2}$. Analyzing the kite in Figure 5(a), we conclude that the area of the upper triangle is $\frac{\pi}{2}$. As $8\frac{\pi}{2} = Area\left(S^2\right)$, it follows that each hypothetical f-tiling in this case must have less than eight kites.

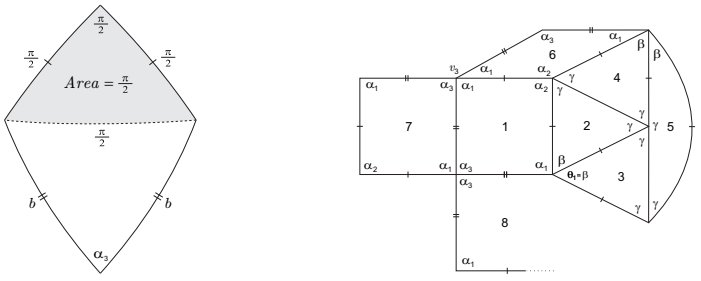

(a) (b)

Figure 5: *Local configurations*

The configuration of Figure 4(a) extends in a unique way to the one illustrated in Figure 5(b). At vertex v_3 we must have $\alpha_1 + k\alpha_3 = \pi$, $k \geq 1$. Since any configuration

must have less than eight kites, we have necessarily $k = 1$. Nevertheless, there is no way to avoid more than eight kites, as illustrated in Figure 6(a).

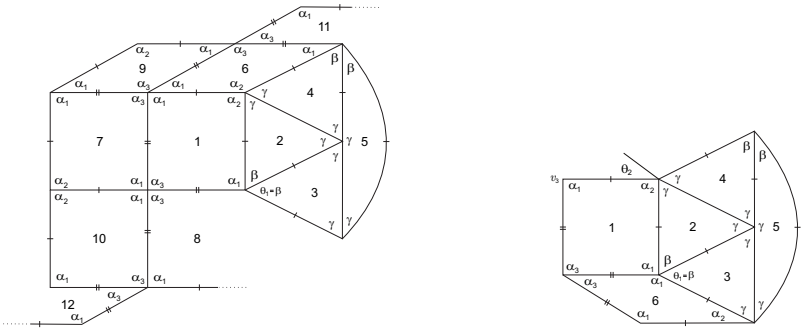

(a) (b)

Figure 6: *Local configurations*

2.2. Suppose now that $\alpha_2 < \frac{\pi}{2}$.

2.2.1. Firstly, we consider

$$\begin{cases} \alpha_1 + \beta = \pi \\ \alpha_2 + \gamma < \pi \end{cases}.$$

With the labeling of Figure 6(b), we must have $\theta_2 = \alpha_2$ (note that $\theta_2 = \beta$ implies a sum of alternate angles containing α_1 and γ at vertex v_3, which is not possible). Taking into account the edge lengths, at vertex v_3 (see Figure 7(a)) we have $\alpha_1 + k\alpha_3 = \pi$, $k \geq 1$.

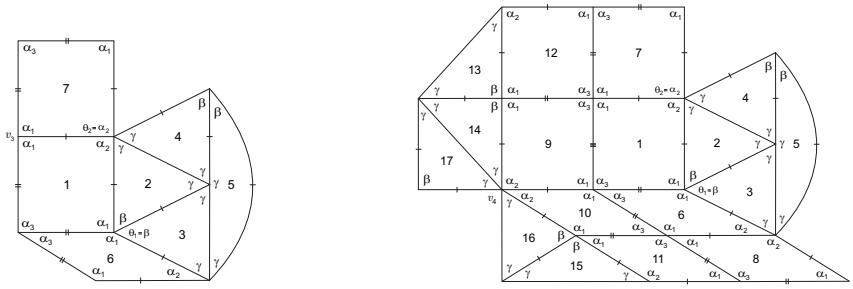

(a) (b)

Figure 7: *Local configurations*

If $k = 1$, the previous configuration extends in a unique way to the one illustrated in Figure 7(b). At vertex v_4 we reach a contradiction as $\alpha_2+\gamma < \pi$ and $\alpha_2+\gamma+\gamma > \pi$ (a condition imposed by the edge lengths).

On the other hand, if $k > 1$ (Figure 8(a)), we also reach a contradiction at vertex v_5, as $\alpha_1 + \alpha_3 + \rho > \pi$, for all $\rho \in \{\alpha_1, \alpha_2, \beta\}$ (note that tile 8 arises in a similar way to tile 7).

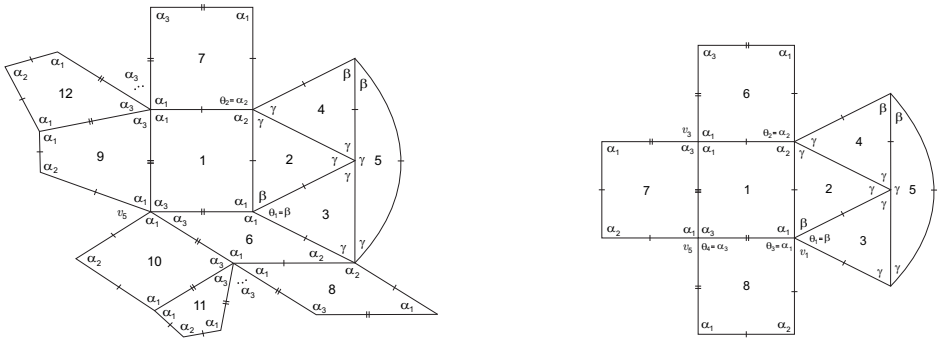

(a) (b)

Figure 8: *Local configurations*

2.2.2. Consider now that

$$\begin{cases} \alpha_1 + \beta < \pi \\ \alpha_2 + \gamma < \pi \end{cases}.$$

Analogously to the previous case, we have $\theta_2 = \alpha_2$ (Figure 8(b)). Note that if $\theta_3 = \alpha_3$ (tile 8), we get $\theta_4 = \alpha_1$ and an incompatibility at vertex v_5 cannot be avoided. Analyzing the edge lengths, at vertices v_1 and v_3 we must have $\alpha_1 + t\beta = \pi$, $t \geq 2$, and $\alpha_1 + k\alpha_3 = \pi$, $k \geq 1$, respectively.

If $k = 1$, the previous configuration extends in a unique way to the one illustrated in Figure 9(a). As previously, at vertex v_6 we reach a contradiction since $\alpha_2 + \gamma < \pi$ and $\alpha_2 + \gamma + \gamma > \pi$. The case $k > 1$ leads to an absurd at vertex v_7 (see Figure 9(b)), as there is no way to satisfy the angle-folding relation around this vertex. □

Proposition 2. *If $\alpha_2 > \alpha_1, \alpha_3$, then $\Omega(K, T)$ is an empty set.*

Proof. In this case, it follows that $\alpha_2 > \frac{\pi}{2}$ and again $c < a < b$. According to Figure 10(a), we analyze separately the cases

$$\alpha_2 + \gamma < \pi \quad \text{and} \quad \alpha_2 + \gamma = \pi.$$

1. If $\alpha_2 + \gamma < \pi$ (note that $\gamma < \frac{\pi}{2} < \alpha_2$), it follows that $\alpha_2 + \gamma + k\alpha_3 = \pi$, $k \geq 1$.

Taking into account the edge lengths, we get $\alpha_2 + \gamma + k\alpha_3 = \pi = \gamma + \alpha_1 + (k - 1)\alpha_3 + \alpha_1 > 3\gamma > \pi$, which is a contradiction.

2. Suppose now that $\alpha_2 + \gamma = \pi$ (Figure 10(b)). We have

$$\alpha_2 > \alpha_1 > \gamma > \beta.$$

According to this relation and side lengths, θ cannot be α_2 or α_3. It also cannot be γ, otherwise we get $\alpha_1 + \gamma + k\alpha_3 = \pi$, $k \geq 1$, and consequently there is no way to satisfy the angle-folding relation around vertex v_1. The same argument applies to the case $\theta = \beta$ (Figure 11), which implies an absurdity at vertex v_2 (we would have $\gamma + \gamma + k\alpha_3 = \pi$, $k \geq 1$, which is not possible). But then $\theta = \alpha_1$,

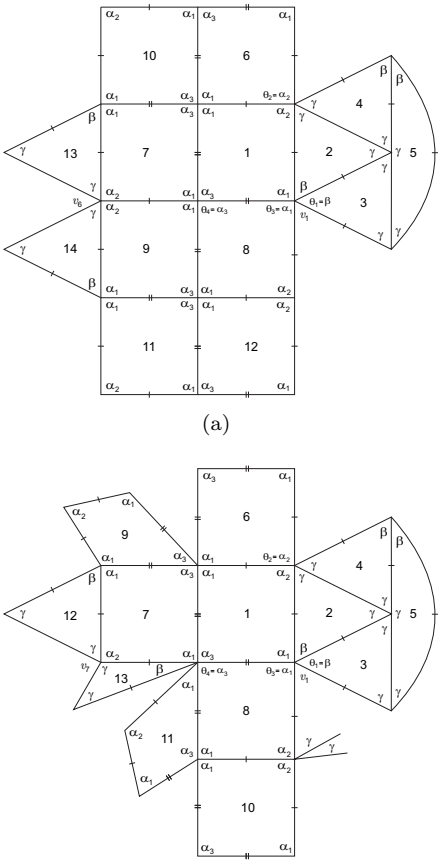

Figure 9: *Local configurations*

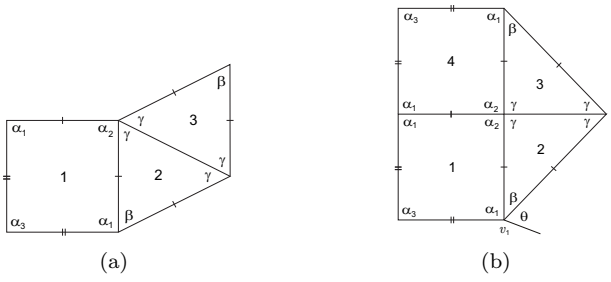

Figure 10: *Local configurations*

and so $\alpha_1 + \alpha_1 + k\alpha_3 = \pi$, $k \geq 0$. The other sum of alternate angles must be $\beta + (k+1)\alpha_3 = \pi$. It follows that $\alpha_1 + \alpha_1 = \beta + \alpha_3$ and $\alpha_2 > \alpha_3 > \alpha_1 > \gamma > \beta$. Therefore, $k = 0$, i.e., $\alpha_1 + \alpha_1 = \pi = \beta + \alpha_3$. As $\alpha_2 + \gamma = \pi$, these conditions contradict our assumptions that $\gamma > \beta$ and $\alpha_2 > \alpha_3$. □

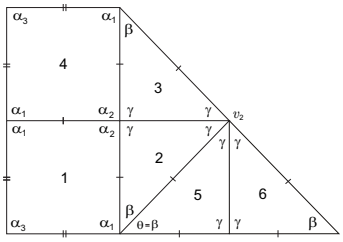

Figure 11: *Local configuration*

2.2. $\gamma < \beta$

As $\gamma < \beta$, we have $\beta > \frac{\pi}{3}$ and $a = d < b, c$. In the next propositions we consider separately each of the following situations:

$$\alpha_1 \geq \alpha_2 > \alpha_3, \quad \alpha_2 > \alpha_1 \geq \alpha_3 \quad \text{and} \quad \alpha_2 > \alpha_3 > \alpha_1.$$

Proposition 3. *If $\alpha_1 \geq \alpha_2 > \alpha_3$, then $\Omega(K,T)$ is an empty set.*

Proof. Suppose that any element of $\Omega\,(K,T)$ has at least two cells congruent to K and T, respectively, such that they are in adjacent positions as illustrated in Figure 2$-I$ and $\alpha_1 \geq \alpha_2 > \alpha_3$ $\left(\alpha_1 > \frac{\pi}{2}\right)$. With the labeling of Figure 12(a), we have

$$\theta_1 = \gamma \quad \text{or} \quad \theta_1 = \beta.$$

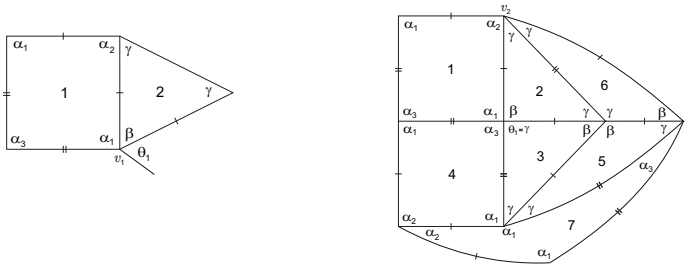

(a) (b)

Figure 12: *Local configurations*

1. Suppose firstly that $\theta_1 = \gamma$.

1.1. If $\alpha_1 + \gamma = \pi$ at vertex v_1, then $b = c$, $\alpha_3 + \beta = \pi$, and we get the configuration illustrated in Figure 12(b). At vertex v_2 we have $\alpha_2 + \gamma = \pi$ or $\alpha_2 + \gamma < \pi$.

If $\alpha_2 + \gamma = \pi$, then $\alpha_1 = \alpha_2 = \beta > \gamma = \alpha_3$ (Figure 13(a)). Although a complete planar representation was possible to draw, we may conclude that such a configuration cannot be realized by an f-tiling. In fact, the dark line is a great circle and has length 2π (v_N and v_S are in antipodal positions since there exist two distinct geodesics of the same length joining them), and so $2a + b = \pi$. Taking into account that tiles 2 and 3 form a spherical lune, we also conclude that $a + b = \pi$, which leads to a contradiction.

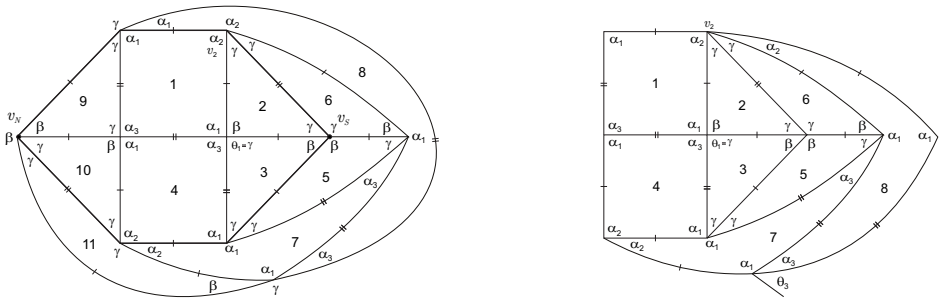

(a) (b)

Figure 13: *Local configurations*

On the other hand, if $\alpha_2 + \gamma < \pi$ (Figure 13(b)), then $\alpha_1 = \beta > \alpha_2 > \gamma = \alpha_3$ and $\theta_3 = \alpha_3$ or $\theta_3 = \gamma$. As we can observe in Figure 14(a), if $\theta_3 = \alpha_3$, there is no way to satisfy the angle-folding relation around vertex v. If $\theta_3 = \gamma$, Figure 14(b) illustrates that analogously to the case $\alpha_2 + \gamma = \pi$, we get $2a + b = \pi$, which is not possible.

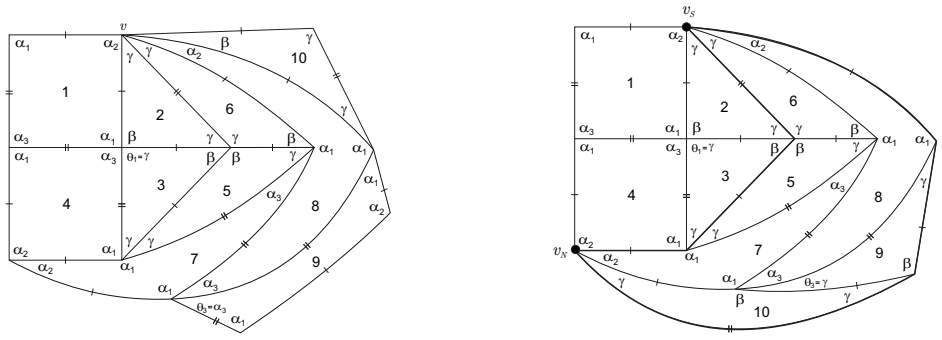

(a) (b)

Figure 14: *Local configurations*

1.2. If $\alpha_1 + \gamma < \pi$ ($\gamma < \frac{\pi}{2} < \alpha_1$), then $\alpha_1 + \gamma + k_1\alpha_3 + k_2\gamma = \pi$, with $k_1, k_2 \geq 0$ and $k_1 + k_2 \geq 1$.

If $c \neq b$ (Figure 15(a)), one of the sum of alternate angles at vertex v_1 must contain $\beta + \gamma + \gamma > \pi$, which is not possible. Therefore, $c = b$ and, with the labeling of Figure 15(b), we must have

$$\theta_2 = \alpha_1 \quad \text{or} \quad \theta_2 = \gamma \quad \text{or} \quad \theta_2 = \alpha_3.$$

1.2.1. If $\theta_2 = \alpha_1$, it follows that $\alpha_1 + \beta < \pi$, and so $\alpha_1 > \beta$. At vertex v_1, one of the sum of alternate angles must contain $\alpha_1 + \gamma + \gamma > \pi$, which is an absurd.

1.2.2. If $\theta_2 = \gamma$, we get the configuration illustrated in Figure 16(a), with $\beta + \gamma + k\alpha_3 = \pi$, $k \geq 1$, and $\frac{\pi}{2} < \alpha_1 < \beta$. According to the edge lengths, the other sum of

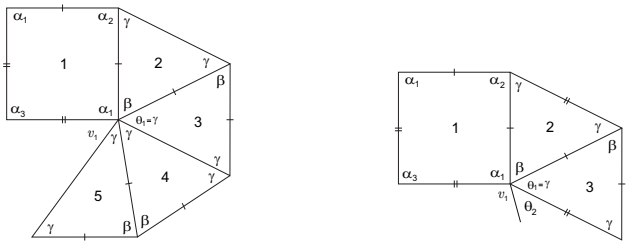

(a) (b)

Figure 15: *Local configurations*

alternate angles at vertex v_1 has to be $\alpha_1+\gamma+\gamma+(k-1)\alpha_3=\pi$. Nevertheless, we obtain a contradiction at vertex v_2 as $\alpha_1+\beta>\pi$.

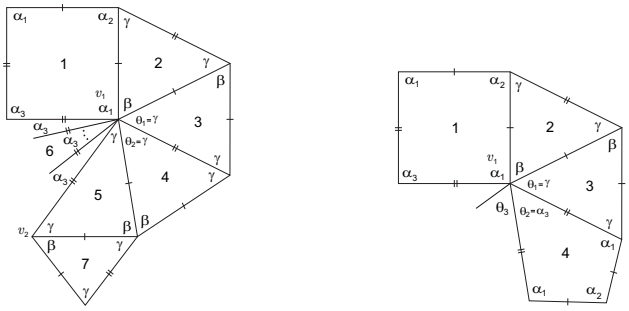

(a) (b)

Figure 16: *Local configurations*

1.2.3. Suppose finally that $\theta_2=\alpha_3$ (see Figure 16(b)). Now, θ_3 must be γ or α_3.

The case $\theta_3=\gamma$ leads to a contradiction. In fact, this condition implies that one of the sum of alternate angles contains $\alpha_1+\gamma+\gamma$ at vertex v_1, and so $\frac{\pi}{2}<\alpha_1<\beta$. The other sum of alternate angles at this vertex will be $\beta+\gamma+k\alpha_3=\pi$, $k\geq 1$, and a similar situation to the previous case arises.

Therefore, $\theta_3=\alpha_3$ and $\alpha_1+\gamma+k\alpha_3=\pi=\beta+(k+1)\alpha_3$, $k\geq 1$, as illustrated in Figure 17(a). We have $\alpha_3<\gamma$, and using the fact that $\alpha_1+\gamma=\beta+\alpha_3$, it follows that $\alpha_3<\gamma<\alpha_2\leq\alpha_1<\beta$. In a sum of alternate angles containing α_1 there can be only angles α_3 or γ (θ_5), and so $\theta_4=\beta$ by the edge lengths. At vertex v_2, we have necessarily $\beta+\gamma=\pi$, otherwise we get $\beta+\gamma+\gamma+k\alpha_3>\pi$, $k\geq 1$ (note that θ_6 cannot be α_1). But we reach a contradiction at vertex v_3, as $\beta+\gamma=\pi>\alpha_1+\gamma$.

2. Consider now that $\theta_1=\beta$ (Figure 12(a)). We analyze separately the cases $\alpha_1+\beta<\pi$ and $\alpha_1+\beta=\pi$.

2.1. If $\alpha_1+\beta<\pi$, we have

$$\alpha_1\geq\alpha_2>\beta>\gamma>\alpha_3$$

and it follows that $\alpha_1+\beta+k\alpha_3=\pi$, $k\geq 1$, as illustrated in Figure 17(b).

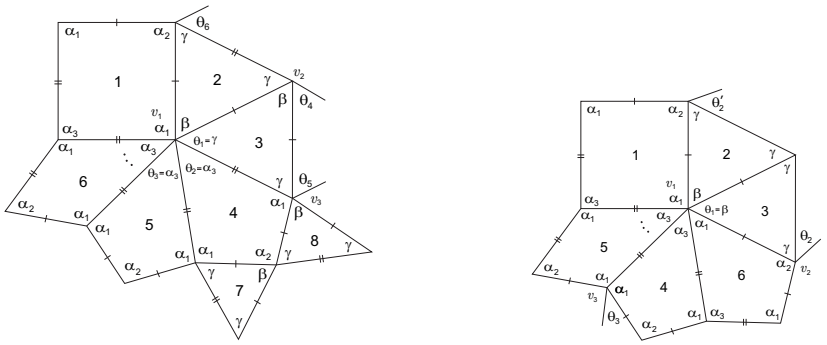

(a) (b)

Figure 17: *Local configurations*

If $c \neq b$, then $\theta_2 = \gamma$ and at vertex v_2 we must have $\alpha_2 + \gamma + t\alpha_3 = \pi$, $t \geq 2$. Taking into account the edge lengths, the other sum of alternate angles comes $\gamma + \alpha_1 + (t-1)\alpha_3 + \alpha_1 > \pi$.

Therefore, $c = b$ and also $\theta_3 = \gamma$ (note that if $\theta_3 = \beta$, at vertex v_3 we would have $\alpha_1 + \beta + k\alpha_3 = \pi = \alpha_1 + \rho_1 + (k-1)\alpha_3 + \rho_2$, with $k \geq 1$ and $\rho_1, \rho_2 \in \{\alpha_1, \gamma\}$; but $\alpha_1 + 2\gamma > \beta + 2\gamma > \pi$). Moreover, $\theta_2 = \gamma$ or $\theta_2 = \alpha_3$.

2.1.1. Suppose firstly that $\theta_2 = \gamma$. Taking into account the angles and side lengths, we have

$$\begin{cases} \alpha_1 + \beta + k\alpha_3 = \pi & \text{(at vertex } v_1\text{)} \\ \alpha_1 + \gamma + t\alpha_3 = \pi & \text{(at vertex } v_3\text{)} \\ \alpha_2 + \gamma + l\alpha_3 = \pi & \text{(at vertex } v_2\text{)} \\ \gamma + \gamma + (l-1)\alpha_3 + \gamma = \pi, \quad l > t > k \geq 1 & \text{(at vertex } v_2\text{)} \end{cases}$$

We have $l > t$ since $\alpha_2 < \alpha_1$; note that $\alpha_2 = \frac{\pi}{2}$ since there are always vertices of valency four, [4]. It follows that $\alpha_2 + \alpha_3 = \gamma + \gamma$, $\alpha_1 = \alpha_2 + (l-t)\alpha_3$, and so $\alpha_1 = 2\gamma + (l-t-1)\alpha_3 \geq 2\gamma$. Using the fact that $\alpha_1 + \beta + k\alpha_3 = \pi$ (vertex v_1), we obtain $\pi = \alpha_1 + \beta + k\alpha_3 \geq 2\gamma + \beta + k\alpha_3 > \pi$, which is an absurd.

2.1.2. Suppose now that $\theta_2 = \alpha_3$ and, by symmetry, $\theta_2' = \alpha_3$. The previous configuration extends to the one illustrated in Figure 18(a). At vertex v_4 we must have $\alpha_1 + \gamma + t\alpha_3 = \pi$, with $t > k \geq 1$. Nevertheless, given the edge lengths, it is not possible.

2.2. If $\alpha_1 + \beta = \pi$ ($\beta < \frac{\pi}{2} < \alpha_1$; see Figure 18(b)), then $\alpha_1 \geq \alpha_2 > \beta > \gamma$ and $\alpha_2 > \alpha_3$.

If $c \neq b$, then $\theta_2 = \gamma$ and at vertex v_2 we must have $\pi = \alpha_2 + \gamma + k\alpha_3 = \gamma + \alpha_1 + (k-1)\alpha_3 + \alpha_1 > \pi$, $k \geq 1$. Then, $c = b$ and also $\theta_2 = \gamma$ or $\theta_2 = \alpha_3$.

2.2.1. Suppose firstly that $\theta_2 = \gamma$. It follows that $\alpha_2 + \gamma + l\alpha_3 = \pi = \gamma + \gamma + (l-1)\alpha_3 + \gamma$, $l \geq 1$, as illustrated in Figure 19(a). We have $\theta_3 = \gamma$ or $\theta_3 = \beta$. In the first case, at vertex v_3 we have $\alpha_1 + \gamma + t\alpha_3 = \pi = \beta + (t+1)\alpha_3$, $t \geq 1$, and so $\alpha_1 + \gamma = \beta + \alpha_3$. As $\alpha_1 > \beta$, it follows $\alpha_3 > \gamma$. Nevertheless, $\pi = \alpha_2 + \gamma + k\alpha_3 >$

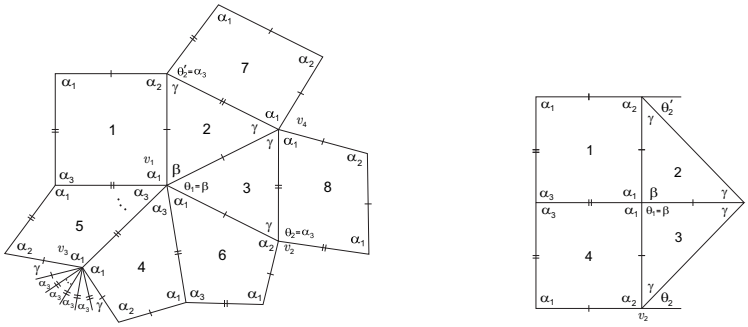

(a) (b)

Figure 18: *Local configurations*

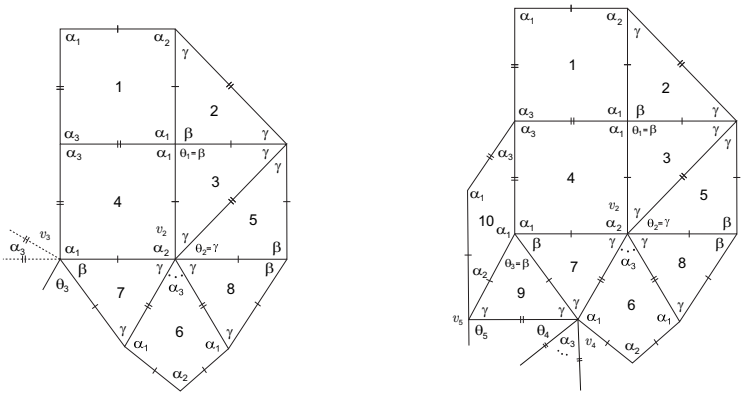

(a) (b)

Figure 19: *Local configurations*

$\alpha_2 + \gamma + k\gamma \geq \alpha_2 + 2\gamma > \beta + 2\gamma > \pi$, which is not possible. Thus, $\theta_3 = \beta$ and the last configuration extends to the one illustrated in Figure 19(b). At vertex v_4 we have $\alpha_1 + \gamma + t\alpha_3 = \pi$, $t \leq l$. Nevertheless, $\theta_4 = \alpha_3$ implies $\theta_5 = \alpha_1$ and then a contradiction cannot be avoided at vertex v_5.

2.2.2. Suppose now that $\theta_2 = \alpha_3$ (Figure 20) and, by symmetry, we also have $\theta_2^{'} = \alpha_3$. At vertex v we must have $\alpha_1 + \gamma + t\alpha_3 = \pi$, $t \geq 1$. However, due to the edge lengths, it is not possible. □

Proposition 4. *If $\alpha_2 > \alpha_1 \geq \alpha_3$, then $\Omega(K,T) \neq \emptyset$ iff*

(i) $\alpha_2 + \gamma = \pi$ and $\alpha_1 = \alpha_3 = \beta = \frac{\pi}{2}$, or

(ii) $\alpha_2 + \gamma = \pi$, $\alpha_1 + \beta = \pi$, $\alpha_3 = \beta$ and $\gamma = \frac{\pi}{3}$.

In the first case, there is a single f-tiling denoted by $\mathcal{G}$. A planar representation is given in Figure 22(b) and a 3D representation is given in Figure 23.

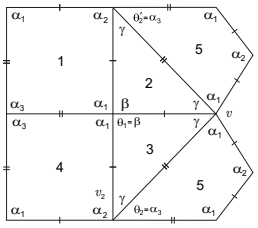

Figure 20: *Local configuration*

In the second case, there is another single f-tiling, $\mathcal{G}^3$. The corresponding planar and 3D representations are given in Figure 26(a) and Figure 26(b), respectively.

Proof. Suppose that any element of $\Omega(K,T)$ has at least two cells congruent to K and T, respectively, such that they are in adjacent positions, as illustrated in Figure 2$-I$ and $\alpha_2 > \alpha_1 \geq \alpha_3$ $\left(\alpha_2 > \frac{\pi}{2}\right)$. Recall that $\beta > \gamma$. With the labeling of Figure 21(a), we have

$$\theta_1 = \gamma \quad \text{or} \quad \theta_1 = \alpha_3.$$

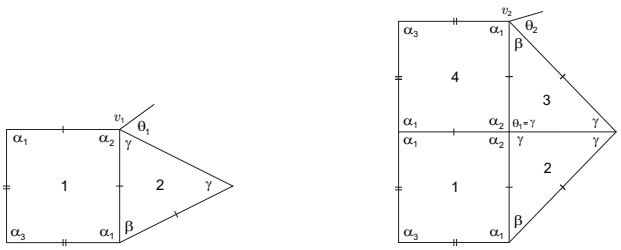

Figure 21: *Local configurations*

1. Suppose firstly that $\theta_1 = \gamma$. We will analyze separately the cases

$$\alpha_2 + \gamma = \pi \quad \text{and} \quad \alpha_2 + \gamma < \pi.$$

1.1. If $\alpha_2 + \gamma = \pi$, it follows that

$$\alpha_2 + \gamma = \pi = \gamma + \rho, \quad \text{with } \rho \in \{\alpha_2, \beta\}.$$

1.1.1. If $\rho = \alpha_2$, then, with the labeling of Figure 21(b), we have $\theta_2 = \alpha_1$, $\theta_2 = \beta$ or $\theta_2 = \gamma$, cases that we analyze separately.

1.1.1.1. If $\theta_2 = \alpha_1$, vertex v_2 may have valency four or greater than four.

1.1.1.1.1. In the first case (Figure 22(a)), if

(i) $\theta_3 = \alpha_2$ and $\alpha_1 + \alpha_3 = \pi$, then $\alpha_2 > \frac{\pi}{2} = \alpha_1 = \alpha_3 = \beta > \gamma > \frac{\pi}{4}$ and the last configuration extends to the planar representation illustrated in Figure 22(b) (note that $\theta_4 = \alpha_3$ leads, by symmetry, to a similar representation). We shall denote such an f-tiling by $\mathcal{G}$. A 3D representation of $\mathcal{G}$ is given in Figure 23.

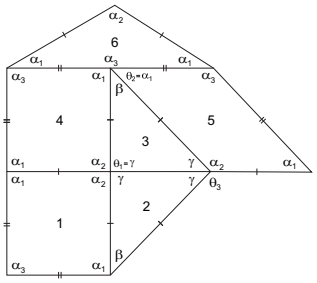

(a)

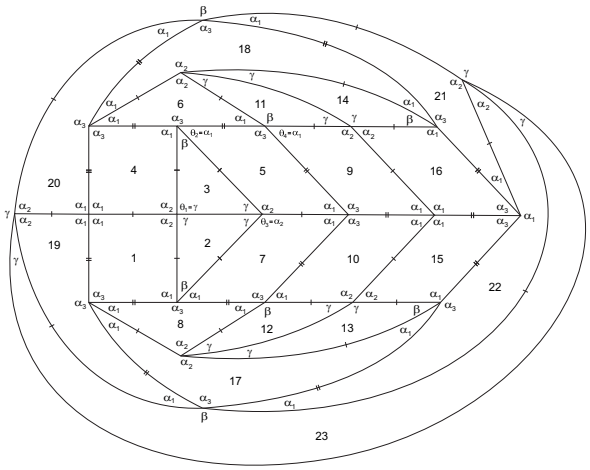

(b) *Planar representation of* $\mathcal{G}$

Figure 22: *Local configurations*

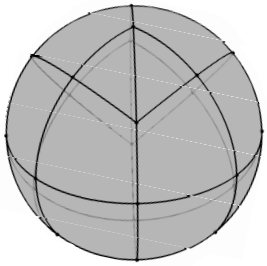

Figure 23: *f-tiling* $\mathcal{G}$

(ii) $\theta_3 = \alpha_2$ and $\alpha_1 + \alpha_3 < \pi$, it follows that $\alpha_2 > \beta > \frac{\pi}{2} = \alpha_1 > \alpha_3 > \gamma$ and $\alpha_1 + k_1\alpha_3 + k_2\gamma = \pi$, with $k_1 \geq 1$, $k_2 \geq 0$ and $k_1 + k_2 \geq 2$. If $k_2 > 0$, then $b = c$, which is not possible. In fact, if $b = c$ and $\alpha_1 = \frac{\pi}{2}, \alpha_3 = \pi - \beta, \gamma =$

$\pi - \alpha_2$ and $\beta, \alpha_2 \in \left(\frac{\pi}{2}, \pi\right)$, we have

$$\begin{cases} \dfrac{\cos\gamma\,(1+\cos\beta)}{\sin\gamma\sin\beta} = \dfrac{\cos\frac{\alpha_3}{2} + \cos\alpha_1\,\cos\frac{\alpha_2}{2}}{\sin\alpha_1\,\sin\frac{\alpha_2}{2}} \\ \dfrac{\cos\beta + \cos^2\gamma}{\sin^2\gamma} = \dfrac{\cos\frac{\alpha_2}{2} + \cos\alpha_1\,\cos\frac{\alpha_3}{2}}{\sin\alpha_1\,\sin\frac{\alpha_3}{2}} \end{cases} \tag{2}$$

$$\iff \quad \begin{cases} \dfrac{-\sin^2\frac{\beta}{2}}{\cos\alpha_2\sin\frac{\alpha_2}{2}} = \dfrac{\sin\alpha_2\cos\frac{\alpha_2}{2}}{\cos\beta + \cos^2\alpha_2} \\ \beta = \arccos\left(\cos\alpha_2 + \sin^2\alpha_2\right) \end{cases}$$

$$\implies \quad \cos^2\alpha_2 - \cos\alpha_2 - 1 = 0 \quad \implies \quad \cos\beta = 0,$$

which is an incongruence.

Therefore, $k_2 = 0$ and we get the configuration illustrated in Figure 24(a). But at vertex v_3 we again obtain an impossibility.

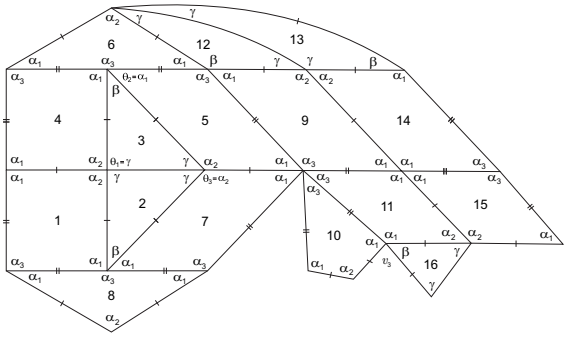

(a)

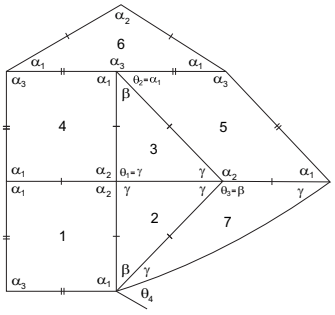

(b)

Figure 24: *Local configurations*

(iii) $\theta_3 = \beta$ (Figure 24(b)), then $\alpha_2 = \beta > \frac{\pi}{2} = \alpha_1 > \alpha_3 = \gamma$ and consequently any choice for θ_4 leads to a contradiction.

1.1.1.1.2. If v_2 has valency greater than four (Figure 21(b)), i.e., $\alpha_1 < \frac{\pi}{2}$, we have $\alpha_2 + \alpha_3 > \pi$, $2\alpha_1 + \alpha_3 > \pi$ and also $\alpha_1 > \frac{\pi}{3}$. Thus, $\alpha_1 + \alpha_1 + k\gamma = \pi$, with $k \geq 1$ (Figure 25(a)).

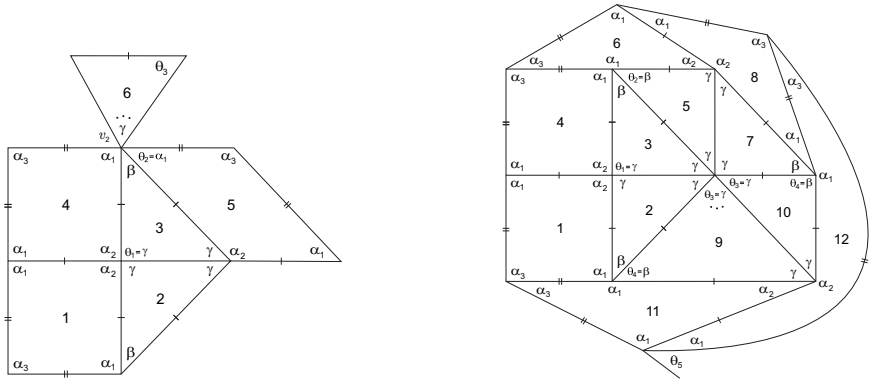

Figure 25: *Local configurations*

According to the edge lengths, both possible choices for θ_3 imply that the other sum of alternate angles becomes $\beta + \alpha_3 + \gamma + (k-1)\rho > \beta + \gamma + \gamma > \pi$, for all $\rho \in \{\alpha_1, \alpha_3, \gamma\}$.

1.1.1.2. If $\theta_2 = \beta$ (Figure 21(b)), we have $\alpha_1 + \beta = \pi$ or $\alpha_1 + \beta < \pi$.

1.1.1.2.1. Suppose that $\alpha_1 + \beta = \pi$.

1.1.1.2.1.1. Consider firstly that $b \neq c$ (Figure 25(b)). Note that $\theta_3 = \alpha_1$ would imply $\theta_4 = \alpha_2$, which is not possible. Now, we have $\theta_5 \in \{\alpha_1, \alpha_3\}$.

If $\theta_5 = \alpha_1$, then $\alpha_1 + \alpha_1 < \pi$. In fact, if $\alpha_1 = \frac{\pi}{2}$, we get $\beta = \frac{\pi}{2}$, $\gamma = \frac{\pi}{3}$ and equation (1) leads to $\alpha_3 > \frac{\pi}{2}$, which is an absurd. Therefore, $\alpha_2 > \beta > \frac{\pi}{2} > \alpha_1 > \gamma > \alpha_3$ (observe that $(\alpha_2+\gamma)+(\alpha_1+\beta)+(\alpha_1+\alpha_1+\rho) = (2\alpha_1+\alpha_2+\alpha_1)+(\beta+\gamma+\rho) > 3\pi$, for all $\rho \in \{\alpha_1, \gamma\}$). However, as $2\alpha_1 + \alpha_2 + \alpha_3 > 2\pi$, we get $2\alpha_1 + \alpha_3 > \pi$.

On the other hand, if $\theta_5 = \alpha_3$ and

(i) $\alpha_1 + \alpha_3 = \pi$, then $\alpha_3 = \beta < \frac{\pi}{2}$, and so $\alpha_2 > \alpha_1 > \frac{\pi}{2} > \beta = \alpha_3 > \gamma = \frac{\pi}{3}$. The last configuration extends to the planar representation illustrated in Figure 26(a). From equation (1) one has $\beta = 4 \arctan \sqrt{\frac{5-2\sqrt{5}}{5}}$. We shall denote such an f-tiling by $\mathcal{G}^3$. A 3D representation of $\mathcal{G}^3$ is given in Figure 26(b).

(ii) $\alpha_1 + \alpha_3 < \pi$, then we have necessarily $k\gamma = \pi$, $k \geq 3$, $\alpha_1 + \bar{k}\alpha_3 = \pi$, $\bar{k} \geq 2$, and the last configuration extends to the one illustrated in Figure 27(a).
At vertex v_3 we have necessarily $\alpha_1 + \alpha_1 = \pi$ and consequently we obtain $\alpha_2 > \frac{\pi}{2} = \alpha_1 = \beta > \gamma = \frac{\pi}{3} > \alpha_3$. By equation (1) it follows that $\alpha_3 = \frac{2\pi}{3}$, which is a contradiction.

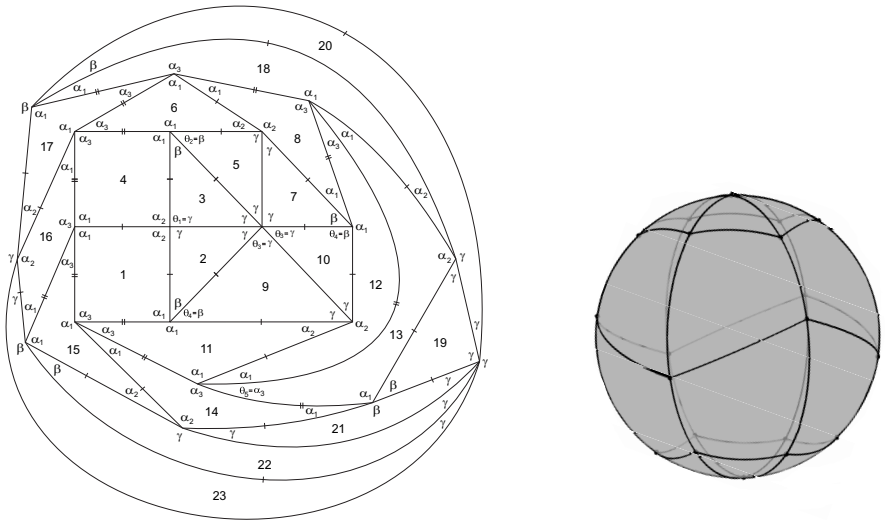

(a) *Planar representation* (b) *3D representation*

Figure 26: *f-tiling* $\mathcal{G}^3$

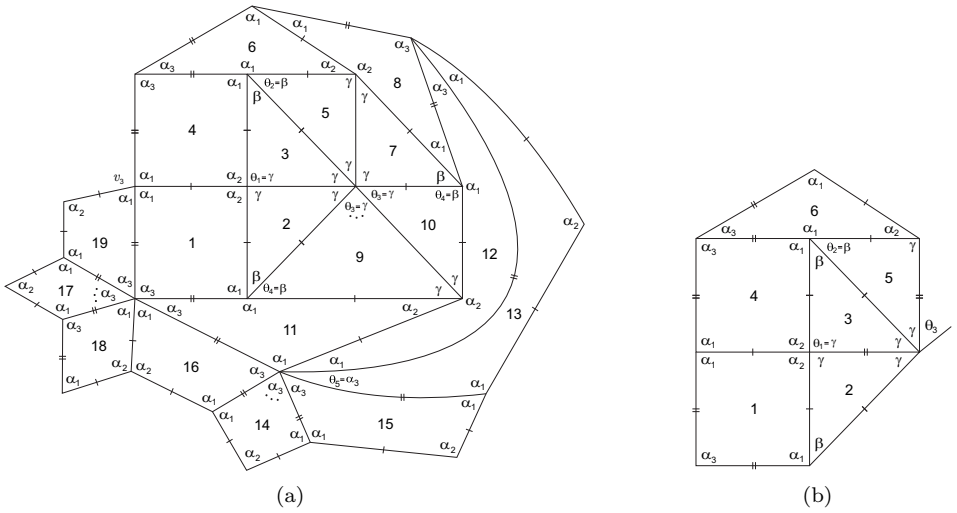

(a) (b)

Figure 27: *Local configurations*

1.1.1.2.1.2. Consider now that $b = c$. With the labeling of Figure 27(b), we have $\theta_3 = \alpha_1$ or $\theta_3 = \gamma$.

The case $\theta_3 = \alpha_1$, illustrated in Figure 28(a), leads to an absurd. In fact, due to vertex v_1 we have $\alpha_2 + \alpha_3 \leq \pi$, which implies $\alpha_1 > \frac{\pi}{2} > \beta$, $\gamma > \frac{\pi}{4}$ and $\gamma \geq \alpha_3$. Consequently, at vertex v_2 we get $\alpha_1 + \gamma + \rho > \pi$, for all $\rho \in \{\alpha_1, \alpha_2, \beta, \gamma\}$.

Using similar arguments, the other case ($\theta_3 = \gamma$) leads to the configuration of

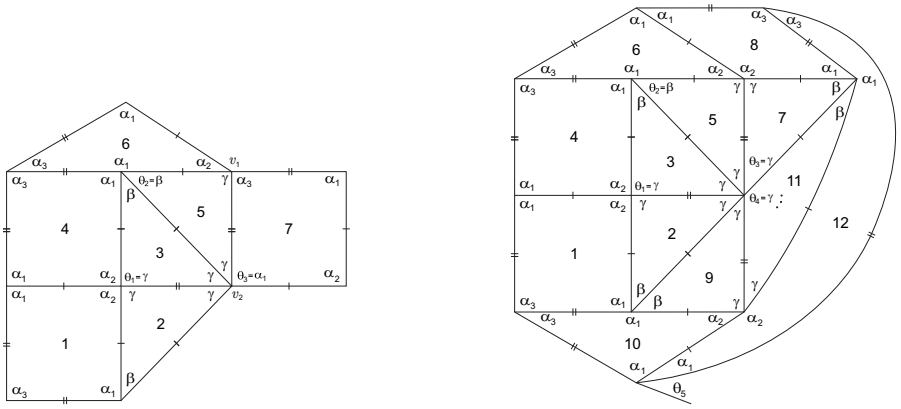

(a) (b)

Figure 28: *Local configurations*

Figure 28(b). We have $k\gamma = \pi$, $k \geq 3$. If $k = 3$, by solving system (2) we get $\gamma = \frac{\pi}{3}$, $\alpha_2 = \frac{2\pi}{3}$, $\alpha_1 = \alpha_3 = 4\arctan\sqrt{-7+2\sqrt{13}} \approx 98.7^\circ$ and $\beta = \pi - \alpha_1 = 2\arctan\sqrt{\dfrac{-5+2\sqrt{13}}{3}} \approx 81.3^\circ$. Nevertheless, according to the angles and edge lengths, any possible choice for θ_5 leads to an absurd. If $k \geq 4$, we have $\gamma \leq \frac{\pi}{4}$, and so $\beta > \frac{\pi}{2} > \alpha_1$, implying $\alpha_2 + \alpha_3 > \pi$ and $\alpha_2 > \beta > \frac{\pi}{2} > \alpha_1 \geq \alpha_3 > \gamma$. In this case we have necessarily $\theta_5 = \gamma$ (Figure 29(a)), as $\alpha_1 + \rho_1 < \pi$ and $\alpha_1 + \rho_1 + \gamma > \pi$, for all $\rho_1 \in \{\alpha_1, \alpha_3\}$. Now, if $\theta_6 = \alpha_1$, then $\theta_7 = \alpha_2$ and we obtain an absurdity at

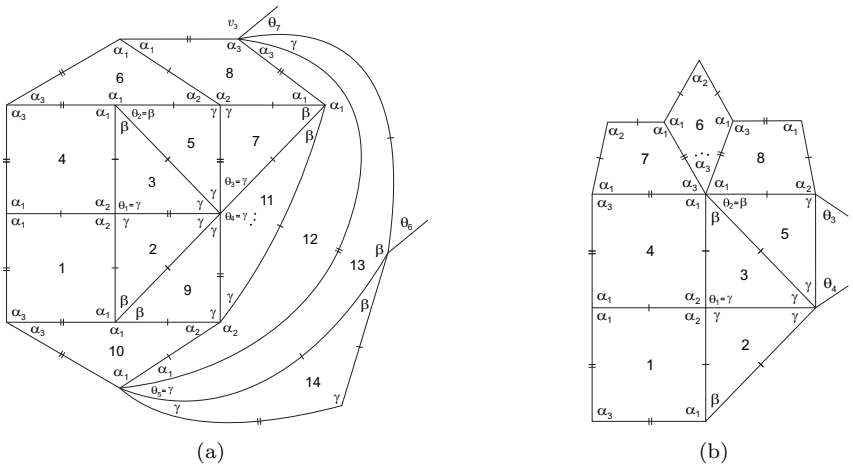

(a) (b)

Figure 29: *Local configurations*

vertex v_3 (Figure 29(a)) since $\alpha_2 + \alpha_3 > \pi$. On the other hand, if $\theta_6 = \gamma$, we have $\beta + \gamma < \pi$ and $\beta + \gamma + \gamma > \pi$.

1.1.1.2.2. Suppose now that $\alpha_1 + \beta < \pi$. Then, $\alpha_1 + \beta + k\alpha_3 = \pi$, $k \geq 1$, and so

$\alpha_1 > \beta$ (note that $2\alpha_1 + \alpha_3 > \pi$). Consequently, $\alpha_2 > \alpha_1 > \beta > \gamma > \alpha_3$, with $\beta < \frac{\pi}{2}$ and $\gamma > \frac{\pi}{4}$, and we obtain the configuration illustrated in Figure 29(b). We must have $\theta_3 = \gamma$. In fact, if $\theta_3 = \alpha_3$, then $\alpha_2 + \bar{k}\alpha_3 = \pi$, with $\bar{k} \geq 2$, which implies $\alpha_1 > \frac{\pi}{2}$. As in this case $\theta_4 = \alpha_1$, we obtain a contradiction since $\alpha_1 + \gamma < \pi$ and $\alpha_1 + \gamma + \rho > \pi$, for all angle ρ. The condition $\theta_3 = \gamma$ leads to the configuration illustrated in Figure 30(a). But at vertex v_4 we have $\beta + \beta + \bar{\bar{k}}\alpha_3 = \pi = \beta + \rho_1 + \rho_2 + (\bar{\bar{k}} - 1)\alpha_3 > \pi$, for $\bar{\bar{k}} \geq 1$ and all $\rho_1, \rho_2 \in \{\alpha_1, \gamma\}$, which is an incongruence.

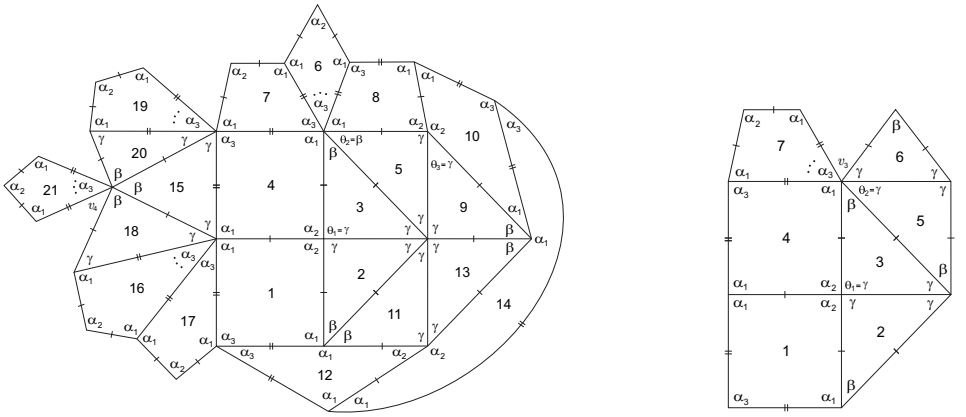

(a) (b)

Figure 30: *Local configurations*

1.1.1.3. Suppose finally that $\theta_2 = \gamma$ (Figure 21(b)).

(i) If $b \neq c$, we must have $\beta+\gamma+k\alpha_3 = \pi$, $k \geq 1$, as illustrated in Figure 30(b). In accordance with the edge lengths, the other sum of alternate angles at vertex v_3 must be of the form $\alpha_1+\gamma+\alpha_1+(k-1)\alpha_3 = \pi$. However, $3\pi = (\alpha_2+\gamma)+(\beta+\gamma+k\alpha_3)+(\alpha_1+\gamma+\alpha_1+(k-1)\alpha_3) > (2\alpha_1+\alpha_2+\alpha_3)+(\beta+\gamma+\gamma) > 3\pi$.

(ii) On the other hand, if $b = c$, we have necessarily $\beta + \gamma + k\alpha_3 = \pi$, $k \geq 1$ (Figure 31). At vertex v_4 we get $\alpha_1+\beta+\bar{k}\alpha_3 = \pi$, $\bar{k} \geq 1$. Taking into account the angles and edge lengths, we conclude that $\theta_3 = \alpha_1$. Consequently, $\theta_4 = \alpha_2$ and an incompatibility at vertex v_5 cannot be avoided.

1.1.2. If $\rho = \beta$, we obtain $\alpha_2 = \beta > \frac{\pi}{2}$ (see Figure 32(a)). Now, we have $\theta_2 = \gamma$ or $\theta_2 = \alpha_3$. In the first case, it follows that $\beta + \gamma = \pi = \alpha_1 + \beta$, which implies that $\alpha_1 = \gamma$. But then $\alpha_2 + \gamma > \pi$, which is an absurd. Therefore $\theta_2 = \alpha_3$ and $\beta + \alpha_3 = \pi$ or $\beta + \alpha_3 < \pi$. If $\beta + \alpha_3 = \pi$, then $\alpha_2 = \beta > \alpha_1 > \alpha_3 = \gamma$ and the other sum of alternate angles at vertex v_2 must be $\alpha_1 + \alpha_1 = \pi$. Nevertheless, $2\pi < 2\alpha_1+\alpha_2+\alpha_3 = (\alpha_1+\alpha_1)+(\alpha_2+\alpha_3) = 2\pi$. On the other hand, if $\beta+\alpha_3 < \pi$, we get $\alpha_2 = \beta > \alpha_1 > \gamma > \alpha_3$ and $\beta + k\alpha_3 = \pi$, $k \geq 2$ (see Figure 32(b)). As $\alpha_2 + \alpha_3 < \alpha_2 + \gamma = \pi$, we obtain $\alpha_1 > \frac{\pi}{2}$. At vertex v_2 it follows that $\beta + k\alpha_3 =$

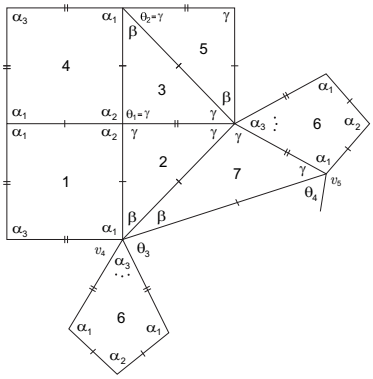

Figure 31: *Local configuration*

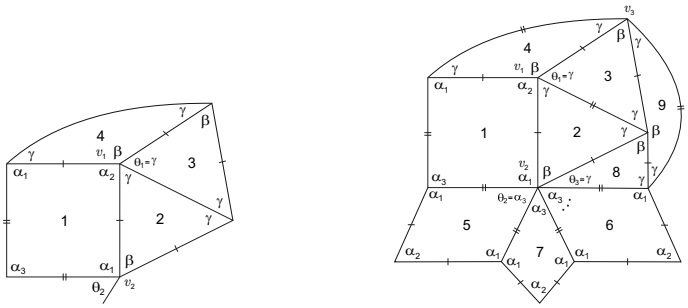

(a) (b)

Figure 32: *Local configurations*

$\pi = \alpha_1 + (k-1)\alpha_3 + \gamma$, i.e., $\theta_3 = \gamma$. At vertex v_3 we must have $\beta + k\alpha_3 = \pi = \gamma + \gamma + (k-1)\alpha_3$, that implies $\alpha_1 = \gamma$, which is not possible.

1.2. Suppose now that $\alpha_2 + \gamma < \pi$ ($\gamma < \frac{\pi}{2} < \alpha_2$). We distinguish the cases

$$\alpha_3 \geq \gamma \quad \text{and} \quad \alpha_3 < \gamma.$$

1.2.1. The condition $\alpha_3 \geq \gamma$ implies $\alpha_2 > \alpha_1 \geq \alpha_3 \geq \gamma$ ($\alpha_1 > \gamma$). As $\beta + \gamma + \gamma > \pi$, any vertex surrounded by an angle β must have valency four. Moreover, $\beta > \alpha_2$ since $\alpha_2 + \gamma + \gamma \leq \pi$. With the labeling of Figure 33(a), θ_2 can be γ or α_3. Both cases lead to a contradiction as

(i) if $\theta_2 = \gamma$, then, according to the edge lengths, $\beta + \gamma = \pi = \alpha_1 + \rho$, with $\rho \in \{\alpha_2, \beta\}$; nevertheless, $\alpha_1 + \beta > \alpha_1 + \alpha_2 > \pi$;

(ii) if $\theta_2 = \alpha_3$, then $\beta + \alpha_3 = \pi = \alpha_1 + \rho$, with $\rho \in \{\alpha_1, \gamma\}$; if $\rho = \alpha_1$, then $2\pi < 2\alpha_1 + \alpha_2 + \alpha_3 = \pi + (\alpha_2 + \alpha_3) < \pi + (\beta + \alpha_3) = 2\pi$; on the other hand, $\rho = \gamma$ implies $\alpha_1 > \alpha_2$, contradicting our initial assumption that $\alpha_2 > \alpha_1 \geq \alpha_3$.

1.2.2. We assume now the condition $\alpha_3 < \gamma$, that implies $\alpha_2 > \alpha_1 > \gamma > \alpha_3$. Taking into account the area of the kite K, we conclude that at least one of the conditions

$\alpha_1 > \frac{\pi}{2}$ or $\alpha_2 + \alpha_3 > \pi$ is verified. As $\alpha_2 + \alpha_3 < \alpha_2 + \gamma < \pi$, then $\alpha_1 > \frac{\pi}{2}$, and consequently $\alpha_2 > \alpha_1 > \frac{\pi}{2} > \gamma > \alpha_3$.

1.2.2.1. If $\beta \geq \alpha_2$, then $\beta \geq \alpha_2 > \alpha_1 > \frac{\pi}{2} > \gamma > \alpha_3$ and as there are always vertices of valency four [4], we must have $\beta + \alpha_3 = \pi$ or $\beta + \gamma = \pi$. Observing Figure 33(a), we conclude that the first case results in a contradiction arising from the fact that there is no way to satisfy the angle-folding relation around vertex v_2.

Thus, $\beta + \gamma = \pi$, and so $\beta > \alpha_2 > \alpha_1 > \frac{\pi}{2} > \gamma > \alpha_3$. As $\theta_2 = \gamma$ (Figure 33(a)) implies an impossibility at vertex v_2, we conclude that $\theta_2 = \alpha_3$ and the configuration extends to the one illustrated in Figure 33(b). At vertex v_2 it follows that $\beta + k\alpha_3 =$

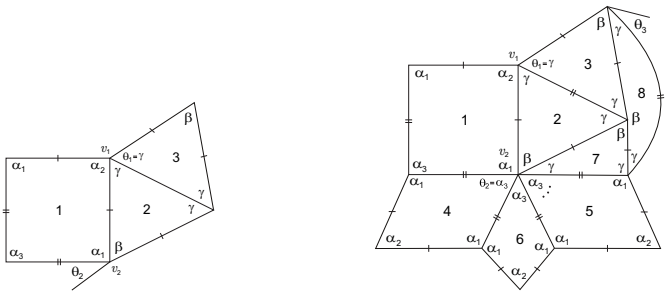

(a) (b)

Figure 33: *Local configurations*

$\pi = \alpha_1 + (k-1)\alpha_3 + \gamma$, $k \geq 3$.

Now, if $\theta_3 = \alpha_3$ (Figure 34(a)), we reach a contradiction at vertex v_3, again resulting from an impossibility to satisfy the angle-folding relation around this vertex (there is no way to complete the sum of alternate angles containing α_2). On the other hand, if $\theta_3 = \gamma$, we get the configuration in Figure 34(b). Observe that the

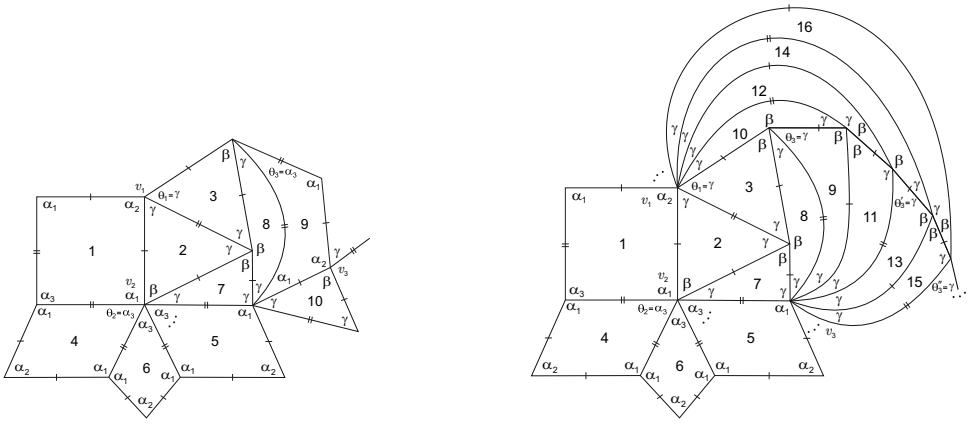

(a) (b)

Figure 34: *Local configurations*

analysis for $\theta_3^{'}, \theta_3^{''}, \ldots$, is analogous to the one made for θ_3. At vertices v_1 and v_3 we reach a contradiction since we obtain $\alpha_1 + t\gamma = \pi$ (around v_3) and $\alpha_2 + t\gamma = \pi$ (around v_1), for some $t \geq 2$ (observe that $\alpha_2 > \alpha_1$).

1.2.2.2. Now we assume that $\beta < \alpha_2$. Recalling that $\alpha_2 > \alpha_1 > \frac{\pi}{2} > \gamma > \alpha_3$, as there must exist vertices of valency four, we have necessarily $\beta + \rho = \pi$, for some $\rho \in \{\alpha_1, \alpha_2, \beta\}$, and so $\alpha_2 > \alpha_1 > \frac{\pi}{2} \geq \beta > \gamma > \frac{\pi}{4} > \alpha_3$. Analyzing the configuration of Figure 35(a), we conclude that $\alpha_2 + \gamma + k\alpha_3 = \pi = \gamma + \theta_2 + (k-1)\alpha_3 + \theta_3$, with $k \geq 1$ and $\theta_2, \theta_3 \in \{\alpha_1, \gamma\}$, at vertex v_1.

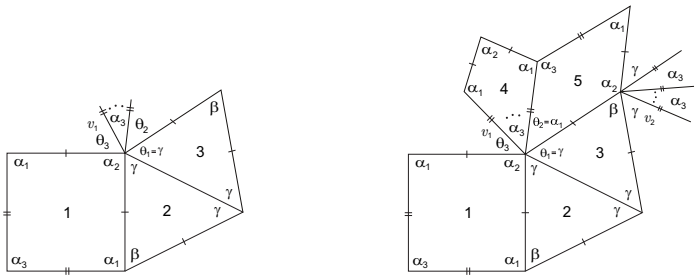

Figure 35: *Local configurations*

If $\theta_2 = \alpha_1$ (see Figure 35(b)), at vertex v_2 we get $\alpha_2 + \gamma + k\alpha_3 = \pi = \beta + \gamma + k\alpha_3$, $k \geq 1$, that implies $\alpha_2 = \beta$, which is a contradiction.

On the other hand, if $\theta_2 = \gamma$, we obtain the configuration of Figure 36(a). Note that if $\theta_3 = \alpha_1$, at vertex v_1 we would have the sum $\alpha_1 + \gamma + \gamma + (k-1)\alpha_3 > \pi$. Therefore, $\theta_3 = \gamma$ and at vertex v_1 we have $\alpha_2 + \gamma + k\alpha_3 = \pi = \gamma + \gamma + \gamma + (k-1)\alpha_3$,

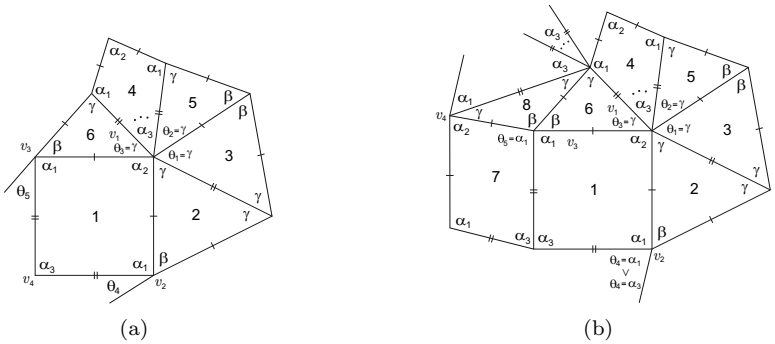

Figure 36: *Local configurations*

$k \geq 1$. According to the side lengths, θ_4 cannot be β or α_2. If $\theta_4 = \gamma$, then $\beta + \gamma + t\alpha_3 = \pi$, with $t > k \geq 1$. Taking into account the side lengths and the angle relations, the sum of alternate angles containing α_1 at vertex v_2 must be of the form $\alpha_1 + \rho_1 + (t-1)\alpha_3 + \rho_2 \geq \alpha_1 + \gamma + (t-1)\alpha_3 + \gamma \geq \alpha_1 + 2\gamma > \frac{\pi}{2} + 2\frac{\pi}{4} = \pi$, for some ρ_1 and ρ_2. Thus, $\theta_4 = \alpha_1$ or $\theta_4 = \alpha_3$ and the same applies to θ_5.

Moreover, if $\theta_4 = \alpha_1$ (or $\theta_5 = \alpha_1$) and $\beta + \alpha_1 < \pi$, then $\beta + \alpha_1 + t\alpha_3 = \pi$, $t \geq 1$, and we reach a contradiction at vertex v_2 using an analogous argumentation as before. On the other hand, we cannot have $\theta_4 = \theta_5 = \alpha_3$, as at vertex v_4 we would have $\alpha_1 + \alpha_1 > \pi$.

The conclusion of the previous discussion is that $(\theta_4, \theta_5) = (\rho, \alpha_1)$, with $\rho \in \{\alpha_1, \alpha_3\}$, or $(\theta_4, \theta_5) = (\alpha_1, \alpha_3)$, and $\alpha_1 + \beta = \pi$ ($\beta < \frac{\pi}{2} < \alpha_1$). Both cases lead to contradictions, as illustrated in Figure 36(b) (vertex v_4) and Figure 37(a) (vertex v_3), respectively.

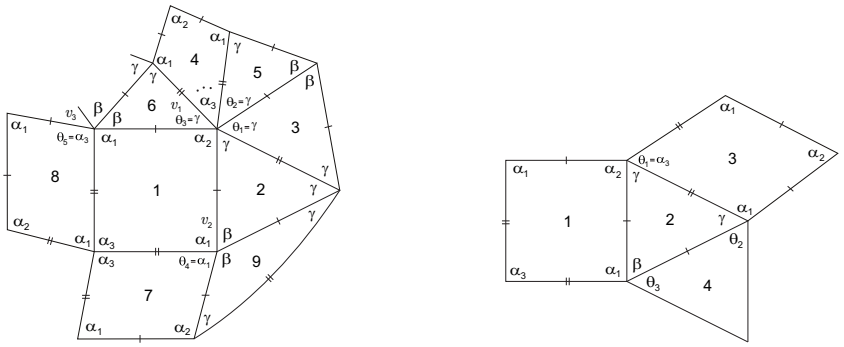

Figure 37: *Local configurations*

2. Suppose finally that $\theta_1 = \alpha_3$ (Figure 37(b)). As $\alpha_2 + \alpha_3 \leq \pi$, we get $\alpha_1 > \frac{\pi}{2}$.

We have $\theta_2 = \beta$ or $\theta_3 = \beta$, and so $\alpha_1 + \beta \leq \pi$, implying $\beta < \frac{\pi}{2}$ and $\gamma > \frac{\pi}{4}$. Thus,

$$\alpha_2 > \alpha_1 > \frac{\pi}{2} > \beta > \gamma > \frac{\pi}{4}.$$

Suppose that $\alpha_1 + \beta < \pi$. Whenever there is a sum of alternate angles containing an angle α_1, it must be of the form $\alpha_1 + \beta + k\alpha_3 = \pi$, $\alpha_1 + \gamma + k\alpha_3 = \pi$ or $\alpha_1 + k\alpha_3 = \pi$, $k \geq 1$, i.e., the number of angles α_3 is greater than or equal to the number of angles α_1. Nevertheless, this is an absurd, as the number of angles α_1 is twice the number of angles α_3 in every f-tiling, and therefore $\alpha_1 + \beta = \pi$. It remains to observe that, under this condition, the cases $\theta_2 = \beta$ or $\theta_3 = \beta$ lead to an absurd. In both cases (see Figures 38(a) and 38(b), respectively), at vertex v_1 one of the sum of alternate angles would be greater than π. □

Proposition 5. *If $\alpha_2 > \alpha_3 > \alpha_1$, then for each $k \geq 4$ there is a single folding tiling, $\mathcal{G}^k$, such that $\alpha_2 + \gamma = \pi$, $\alpha_1 + \alpha_3 = \pi = \alpha_1 + \beta$, $\gamma = \frac{\pi}{k}$ and $\beta = 2\arccos\left(\frac{1+\sqrt{5}}{2}\sin\frac{\pi}{2k}\right)$. A planar representation and 3D representations for $k = 4$ and $k = 5$ are illustrated in Figures 41(b) and 42, respectively.*

Proof. Suppose that any element of $\Omega(K, T)$ has at least two cells congruent to K and T, respectively, such that they are in adjacent positions, as illustrated in

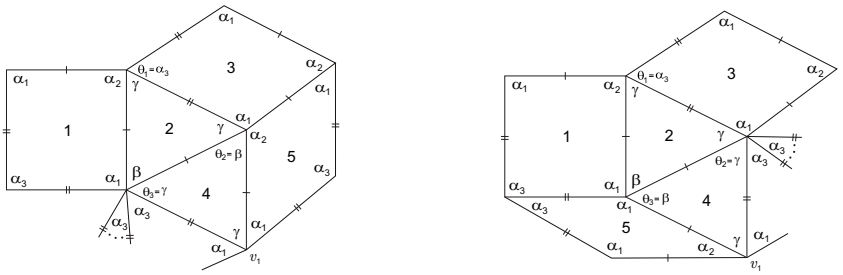

Figure 38: *Local configurations*

Figure $2-I$ and $\alpha_2 > \alpha_3 > \alpha_1$. As $\alpha_2 + \alpha_i > \pi$, for all $i = 1, 2, 3$, we obtain the configuration illustrated in Figure 39(a) and the relations

$$\alpha_2 > \alpha_3 > \alpha_1 > \gamma \quad \text{and} \quad \alpha_2 > \frac{\pi}{2} > \gamma.$$

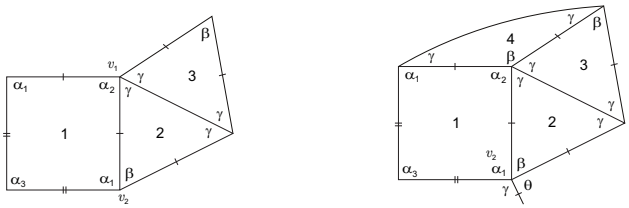

Figure 39: *Local configurations*

We will distinguish the cases

$$\alpha_2 + \gamma = \pi \quad \text{and} \quad \alpha_2 + \gamma < \pi.$$

1. Suppose firstly that $\alpha_2 + \gamma = \pi$. Then, at vertex v_1 we have $\alpha_2 + \gamma = \pi = \gamma + \rho$, with $\rho \in \{\beta, \alpha_2\}$.

The case $\rho = \beta$ leads to an absurd at vertex v_2, as illustrated in Figure 39(b), since $\alpha_1 + \theta > \pi$ (observe that θ must be α_2 or β).

On the other hand, if $\rho = \alpha_2$, as $\beta + 2\gamma > \pi$, $\alpha_2 > \alpha_3 > \alpha_1 > \gamma$ and $\beta > \gamma$, we must have $\beta + \theta = \pi$, with $\theta \in \{\gamma, \alpha_3, \alpha_1\}$, at vertices v_2 and v_3 (see Figure 40(a)).

If $\beta + \gamma = \pi$ (vertex v_2), i.e., $\theta = \gamma$, we get $\alpha_2 = \beta$ and it follows that $\beta + \gamma = \pi = \alpha_1 + \rho$, with $\rho \in \{\beta, \alpha_2\}$, which is a contradiction.

If $\beta + \alpha_3 = \pi$ (vertex v_2), then the other sum of alternate angles at vertex v_2 must be $\alpha_1 + \alpha_1 = \pi$, and so $\alpha_1 > \alpha_3 > \alpha_1 = \frac{\pi}{2} > \beta > \gamma$. The previous configuration extends to the one illustrated in Figure 40(b) (note that $\alpha_3 + \gamma < \pi$ and $\alpha_3 + 2\gamma > \pi$), yielding an absurd at vertex v_4.

If $\beta + \alpha_1 = \pi$ (vertex v_2), we get the configuration of Figure 41(a). We must have $\beta > \alpha_1$. In fact, the condition $\alpha_1 \geq \beta$ implies $\frac{\pi}{2} \geq \beta > \gamma > \frac{\pi}{4}$ and, as $k\gamma = \pi$,

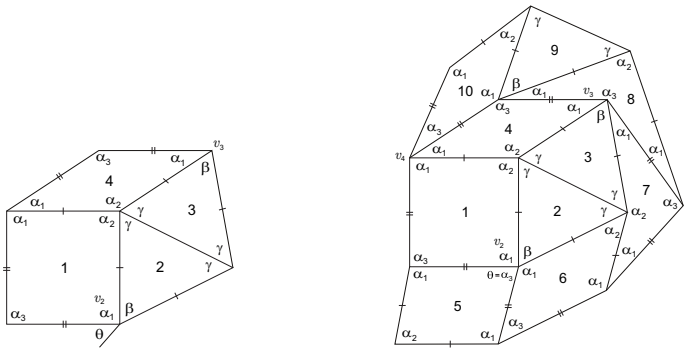

(a) (b)

Figure 40: *Local configurations*

we have $\gamma = \frac{\pi}{3}$. At vertex v_4 we reach a contradiction since $\alpha_3 + \rho > \pi$, for all $\rho \in \{\alpha_1, \alpha_2, \alpha_3, \beta\}$, $\alpha_3 + \gamma < \pi$ and $\alpha_3 + \gamma + \gamma > \pi$.

Therefore $\alpha_2 > \alpha_3 > \alpha_1 > \gamma$ and $\beta > \frac{\pi}{2} > \alpha_1$. At vertex v_4 we have $\theta_4 \in \{\alpha_1, \alpha_3, \gamma\}$.

(i) If $\theta_4 = \alpha_1$, the last configuration extends to the planar representation illustrated in Figure 41(b). For each $k \geq 4$ we obtain a closed planar configuration. Such configuration corresponds to an f-tiling $\mathcal{G}^k$ in which $\beta = 2 \arccos\left(\frac{1+\sqrt{5}}{2} \sin\frac{\pi}{2k}\right)$. 3D representations of $\mathcal{G}^4$ and $\mathcal{G}^5$ are given in Figure 42.

(ii) If $\theta_4 = \alpha_3$, then $\alpha_2 > \beta > \frac{\pi}{2} \geq \alpha_3 > \alpha_1 > \gamma$. As $\alpha_3 + \alpha_3 + \rho > \pi$, for all $\rho \in \{\alpha_1, \alpha_2, \alpha_3, \beta, \gamma\}$, we conclude that $\alpha_3 = \frac{\pi}{2}$ (Figure 43(a)). At vertex v_5 we have necessarily $\alpha_1 + \alpha_1 + k\gamma = \pi$ since $\alpha_1 + \alpha_1 + \alpha_1 = \pi$ implies that system (2) has no solution and $\alpha_1 + \alpha_1 + \alpha_1 + \gamma > \pi$. We also have $b \neq c$, otherwise system (2) has no solution, and so the previous configuration extends to the one illustrated in Figure 43(b). But a contradiction at vertex v_6 is impossible to avoid.

(iii) Finally, if $\theta_4 = \gamma$, we must have $\alpha_3 + k\gamma = \pi$, with $k \geq 2$ (Figure 44). Taking into account the angles and edge lengths, there is no way to satisfy the angle-folding relation around vertices v_5 and v_6.

2. Suppose now that $\alpha_2 + \gamma < \pi$ (Figure 39(a)); $\gamma < \frac{\pi}{2} < \alpha_2$). As $\beta + 2\gamma > \pi$, we conclude that $\beta > \alpha_2$, and consequently at vertex v_2 we must have $\beta + \gamma = \pi$. Nevertheless, there is no way to satisfy the angle-folding relation around this vertex. □

Concerning to the combinatorial structure of each tiling obtained before, we follow the notation used in previous papers. Any symmetry of $\mathcal{G}^k$, $k \geq 3$, fixes $N = (0, 0, 1)$ (and consequently $S = -N$) or maps N into S (and consequently S into N). The symmetries that fix N are generated, for instance, by the rotation $R^z_{\frac{2\pi}{k}}$

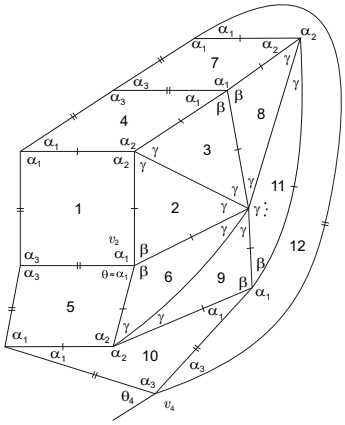

(a)

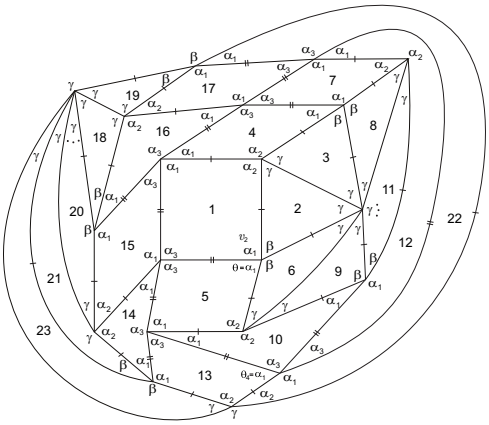

(b) *Planar representation of* $\mathcal{G}^k$

Figure 41: *Local configurations*

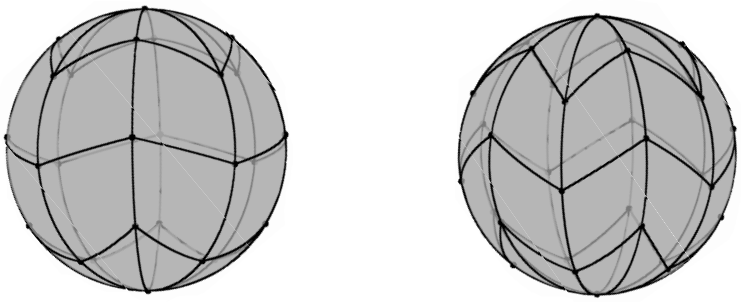

Figure 42: *f-tilings* $\mathcal{G}^k$*, cases* $k = 4$ *and* $k = 5$

(around the z axis) and the reflection ρ^{yz} (on the coordinate plane yoz), giving rise

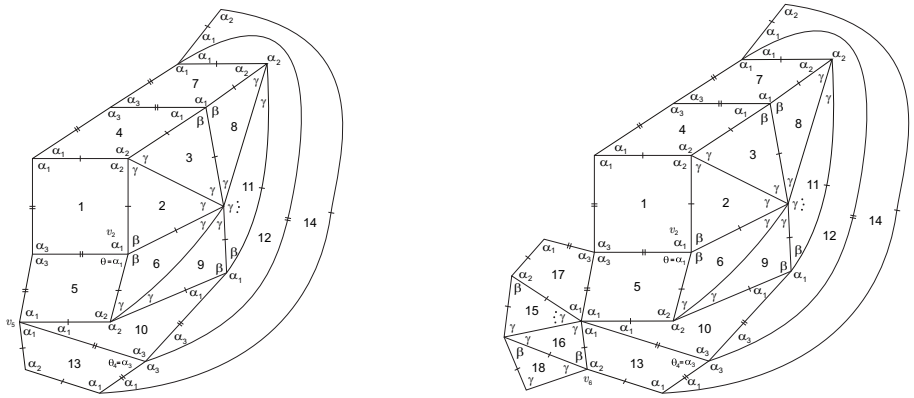

(a) (b)

Figure 43: *Local configurations*

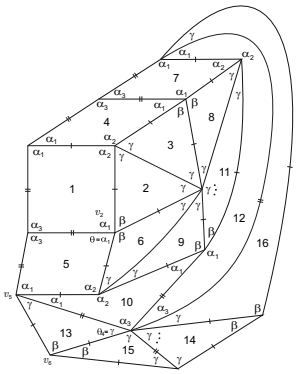

Figure 44: *Local configuration*

to a subgroup of $G(\mathcal{G}^k)$ isomorphic to D_k (the dihedral group of order $2k$). Now, the map $\phi = R^z_{\frac{\pi}{k}} \circ \rho^{xy}$ is a symmetry of $\mathcal{G}^k$ that permutes N and S allowing us to get all the symmetries that map N into S. One has $\phi^{2k-1} \circ \rho^{yz} = \rho^{yz} \circ \phi$ and ϕ has order $2k$. It follows that ϕ and ρ^{yz} generate $G(\mathcal{G}^k)$. And so it is isomorphic to D_{2k}.

Similarly, we conclude that the symmetry group of $\mathcal{G}$ is D_4.

3. Main theorem

In the previous section, we have proved the following main result.

Theorem 1. *If K and T are a spherical kite and an isosceles spherical triangle of internal angles $(\alpha_1, \alpha_2, \alpha_1, \alpha_3)$, and (β, γ, γ), respectively, in case of adjacency I (Figure 2-I), then $\Omega(K, T)$ is composed of a single tiling $\mathcal{G}$ and a discrete family $\mathcal{G}^k$, $k \geq 3$, with a combinatorial structure presented in Table 1. Our notation is as follows:*

- $\gamma_0 = 2\arcsin\frac{-\sqrt{2}(1-\sqrt{5})}{4}$; *$\beta_0^k$ is the solution of equation (1), with* $\alpha_1 = \pi - \beta_0^k$, $\alpha_2 = \pi - \gamma$, $\alpha_3 = \beta_0^k$ *and* $\gamma = \frac{\pi}{k}$, *with* $k \geq 3$.
- $|V|$ *is the number of distinct classes of congruent vertices;*
- N_1 *is the number of kites congruent to* K *and* N_2 *is the number of triangles congruent* T *(used in the dihedral f-tilings);*
- $G(\tau)$ *is the symmetry group of each tiling* $\tau \in \Omega(K, T)$.

f-tiling	$\boldsymbol{\alpha_1}$	$\boldsymbol{\alpha_2}$	$\boldsymbol{\alpha_3}$	$\boldsymbol{\beta}$	$\boldsymbol{\gamma}$	$\lvert V\rvert$	N_1	N_2	$G(\tau)$
$\boldsymbol{\mathcal{G}}$	$\frac{\pi}{2}$	$\pi - \gamma_0$	$\frac{\pi}{2}$	$\frac{\pi}{2}$	γ_0	4	8	16	D_4
$\boldsymbol{\mathcal{G}^k}$, $\boldsymbol{k \geq 3}$	$\pi - \beta_0^k$	$\pi - \gamma$	β_0^k	β_0^k	$\frac{\pi}{k}$	4	$4k$	$4k$	D_{2k}

Table 1: *Combinatorial structure of dihedral f–tilings of* S^2 *by kites and isosceles triangles in case of adjacency I*

Acknowledgement

The authors were partially supported by the Portuguese Government through the FCT - Fundação para a Ciência e a Tecnologia with national funds through Centro de Matemática da Universidade de Trás-os-Montes e Alto Douro (PEst-OE/MAT-/UI4080/2014).

References

[1] C. P. AVELINO, A. F. SANTOS, *Spherical and planar folding tessellations by kites and equilateral triangles*, Australas. J. Combin. **53**(2012), 109–125.
[2] A. M. BREDA, *A class of tilings of* S^2, Geom. Dedicata **44**(1992), 241–253.
[3] A. M. BREDA, P. S. RIBEIRO, *Spherical f-tilings by two non congruent classes of isosceles triangles-I*, Math. Commun. **17**(2012), 127–149.
[4] A. M. BREDA, A. F. SANTOS, *Dihedral f-tilings of the sphere by spherical triangles and equiangular well centered quadrangles*, Beiträge Algebra Geom. **45**(2004), 447–461.
[5] A. M. BREDA, A. F. SANTOS, *Dihedral f-tilings of the sphere by rhombi and triangles*, Discrete Math. Theor. Comput. Sci. **7**(2005), 123–140.
[6] A. M. BREDA, P. S. RIBEIRO, A. F. SANTOS, *A Class of Spherical Dihedral F-Tilings*, European J. Combin. **30**(2009), 119–132.
[7] R. J. DAWSON, *Tilings of the sphere with isosceles triangles*, Discrete Comput. Geom. **30**(2003), 467–487.
[8] R. J. DAWSON, B. DOYLE, *Tilings of the sphere with right triangles I: the asymptotically right families*, Electron. J. Combin. **13**(2006), #R48.
[9] R. J. DAWSON, B. DOYLE, *Tilings of the sphere with right triangles II: the* $(1, 3, 2)$, $(0, 2, n)$ *family*, Electron. J. Combin. **13**(2006), #R49.
[10] S. A. ROBERTSON, *Isometric folding of riemannian manifolds*, Proc. Royal Soc. Edinb. Sect. A **79**(1977), 275–284.
[11] Y. UENO, Y. AGAOKA, *Classification of tilings of the 2-dimensional sphere by congruent triangles*, Hiroshima Math. J. **32**(2002), 463–540.